

Published in final edited form as:

Brain Res. 2014 July 29; 1574: 6–13. doi:10.1016/j.brainres.2014.06.013.

Altered discharges of spinal neurons parallel the behavioral phenotype shown by rats with bortezomib related chemotherapy induced peripheral neuropathy

Caleb R. Robinson, Hongmei Zhang, and Patrick M. Dougherty

Department of Anesthesia and Pain Medicine Research, The University of Texas M.D. Anderson Cancer Center, Houston, Texas

Abstract

Bortezomib is a first generation proteasome inhibitor that is the frontline chemotherapy for multiple myeloma with the chief dose-limiting side effect of painful peripheral neuropathy. The goal of this study was to define the behavioral phenotype in a preclinical model of bortezomib chemotherapy-induced peripheral neuropathy (CIPN) and to test whether this is matched by changes in the physiological responses of spinal wide dynamic range neurons. Sprague-Dawley rats were treated with four injections of bortezomib at four doses, 0.05mg/kg, 0.10 mg/kg, 0.15 mg/kg, 0.20 mg/kg, or equal volume of saline. All doses of bortezomib above 0.05mg/kg produced showed significant dose-dependent mechanical hyperalgesia that was fully established at 30 days after treatment and that recovered to baseline levels by day 69 after treatment. Thermal, cold, and motor testing were all unaffected by treatment with bortezomib. Spinal wide dynamic range (WDR) neurons in rats with confirmed bortezomib-related CIPN showed an increase in number of evoked discharges to mechanical stimuli and exaggerated after-discharges in rats with bortezomib CIPN.

Keywords

bortezomib; wide dynamic range neurons; chemotherapy-induced peripheral neuropathy

1. Introduction

Bortezomib is a first generation proteasome inhibitor drug used in the treatment of multiple myeloma and other non-solid malignancies. It may be administered on its own, but is used primarily in conjunction with other drugs such as thalidomide, dexamethasone, melphalan, and prednisone (San Miguel et al., 2008; Kaufman et al., 2010). As with many other

© 2014 Elsevier B.V. All rights reserved.

*Correspondence to: Patrick M. Dougherty, Department of Anesthesia and Pain Medicine, The University of Texas M.D. Anderson Cancer Center, Houston, Texas 77030. Tel: 713-745-0438, Fax: 713-792-7591, pdougherty@mdanderson.org.

Disclosures: The authors have no conflicts of interest or other disclosures concerning this work.

Publisher's Disclaimer: This is a PDF file of an unedited manuscript that has been accepted for publication. As a service to our customers we are providing this early version of the manuscript. The manuscript will undergo copyediting, typesetting, and review of the resulting proof before it is published in its final citable form. Please note that during the production process errors may be discovered which could affect the content, and all legal disclaimers that apply to the journal pertain.

chemotherapeutic drugs, bortezomib exhibits a side effect of painful chemotherapy-induced peripheral neuropathy (CIPN) (Aghajanian et al., 2002; Kane et al., 2006). This appears in a stocking and glove distribution with patients reporting the most severe neuropathic symptoms in the glabrous skin of their toes and fingers (Cata et al., 2007). CIPN frequently becomes so severe that patients are given a lower dose than maximally effective or forced off of chemotherapy entirely (Cata et al., 2007; Broyl, Jongen, Sonneveld., 2012). Understanding the mechanisms of chemotherapy-induced peripheral neuropathy so that it may be alleviated or prevented is therefore critical if patients are to have a higher quality of life and benefit fully from chemotherapy treatment.

Bortezomib was granted a fast-track approval by the FDA for use in treatment of multiple myeloma due to its effectiveness. It is distinct from other chemotherapy drugs in that it targets proteasomes within cells, which consist of a 19S subunit that detects ubiquitination and a 20S subunit that degrades ubiquitinated proteins. Bortezomib competitively binds to the 20S subunit, preventing the normal degradation of misfolded or obsolete proteins by targeting the chymotrypsin-like activity of the proteasome (Adams et al., 1999; Adams, 2002; Adams and Kauffman, 2004). Due to high levels of protein turnover and synthesis, the accumulation of these proteins has a greater consequence in cancer cells than in healthy cells. However, it is unclear how this accumulation of proteins results in apoptosis, as multiple mechanisms have been proposed that could explain this effect. Cell cycle arrest may occur when proteins regulating the cell cycle at critical stages remain at concentrations that do not permit proliferating cells to continue through the cell cycle, such as what may occur with stabilization of I κ B, the inhibitory form of the transcription factor NF κ B (Hideshima et al., 2001; Voorhees et al., 2003). This would not necessarily account for apoptosis, but could explain a slower progression in treated patients. It is also possible that blocking the cell's ability to digest misfolded or otherwise faulty proteins via bortezomib treatment causes excessive stress on the endoplasmic reticulum, which then leads to caspase-mediated apoptosis (Landowski et al., 2005). Alternatively, bortezomib may trigger apoptosis through the activity of p53, which prompts mitochondrial cytochrome *c*-triggered apoptosis (Hideshima et al., 2003; Voorhees et al., 2003). Malignant cells must continually work against apoptotic signals, and it has been suggested that inhibiting the proteasome shifts this balance in a manner unfavorable to the survival of malignant cells. Many other reasonable mechanisms have been proposed for how proteasome inhibition leads to apoptosis in addition to those listed here. In light of this, it seems likely that there are multiple pathways contributing to apoptosis and inhibited growth of cancer cells treated with bortezomib, as opposed to any single mechanism.

With the current lack of understanding of the activity of bortezomib on cancer cells, it is not surprising that the cause of bortezomib -induced peripheral neuropathy is also not well understood. This poses major difficulties in identifying treatments to prevent or reverse this neuropathy. Understanding the cause of bortezomib CIPN is more complicated than simply treating generalized pain, since CIPN in other drug models does not necessarily affect every modality of somatosensation. Instead, a given drug has a profile of select types of stimuli that produce abnormal numbness, tingling, pain, or other sensations that are similar across drugs, but not identical (Cata et al., 2007; Dougherty et al., 2007; Boyette-Davis et al.,

2012). It is therefore necessary in characterizing bortezomib-induced peripheral neuropathy to survey multiple modalities so as to provide insight as to a common mechanism that may underlie affected modalities.

Electrophysiological data are also important to determine whether central sensitization, glutamate transporter dysfunction, or other similar mechanisms are involved, since bortezomib cannot cross the blood brain barrier (Adams, 2002). Studies with other chemotherapy drug models have revealed increased responses and persistent afterdischarges in wide dynamic range (WDR) neurons in the spinal dorsal horn in CIPN (Cata et al., 2006; Cata, Weng, and Dougherty, 2008a). A similar finding in bortezomib would indicate a maladaptive response in these cells that might explain both exaggerated sensitivity and persistent after sensations to cutaneous stimuli such as those seen in patients (Cata et al., 2007; Boyette-Davis et al., 2011). Taken together with behavioral data, the present study was conducted to identify changes in sensory behavioral phenotype and accompanying spinal cellular responses to understand bortezomib CIPN for the sake of its treatment or prevention.

2. Results

2.1 Mechanical Sensitivity

2.1.1 0.05mg/kg bortezomib—Rats treated at the 0.05mg/kg dose of bortezomib had a gradual and slight onset of mechanical hyperalgesia versus baseline behavior that was determined in ANOVA to not differ significantly versus controls (Fig. 1A). Nevertheless, this group was significantly lower versus control at day 19 (naïve: 17.2 ± 2.49 g, bortezomib: 10.4 ± 1.10 g), as well as at days 23, 26, and 34. After this point, rats began to recover from changes in mechanical sensitivity. Although the average withdrawal threshold was higher for this group at later time points than in saline-treated rats, this difference was not statistically significant, and these rats started with a higher baseline threshold than the saline-treated group.

2.1.2 0.10mg/kg bortezomib—Rats treated at the 0.10mg/kg dose of bortezomib showed a significantly reduced mechanical withdrawal threshold than the saline-treated and 0.05mg/kg treated groups ($P < 0.01$), but not different from the 0.15mg/kg or 0.20mg/kg groups. This group first showed statistically significant mechanical hyperalgesia versus controls at day 6 (naïve: 19.3 ± 2.56 g, bortezomib: 13.9 ± 1.54 g), after the third injection of bortezomib (Fig. 1B). Significant differences were also observed at every following time point until day 54. Peak severity was observed from day 16 to day 34 (approx. 7.5g). Recovery from changes in mechanical sensitivity was gradual after this point, with statistically equivalent behavior versus saline-treated rats at days 63 and 69.

2.1.3 0.15mg/kg bortezomib—Rats treated at the 0.15mg/kg dose of bortezomib showed significantly lowered withdrawal threshold from the saline-treated and 0.05mg/kg group ($P < 0.01$), but not from the 0.10mg/kg or 0.20mg/kg groups. This group first showed statistically significant mechanical hyperalgesia versus controls at day 8 (naïve: 17.3 ± 2.48 g, bortezomib: 11.1 ± 2.41 g), after the final injection of bortezomib (Fig. 1C). Significant differences were also observed at days 12, 19 through 41, and 54. Peak severity was

observed from day 19 to day 34 (approx. 7.5g). Animals began to recover from mechanical hypersensitivity following this point, with statistically equivalent behavior versus saline-treated rats at days 47, 63, and 69.

2.1.4 0.20mg/kg bortezomib—Rats treated at the 0.20mg/kg dose of bortezomib showed significantly lowered withdrawal threshold from the saline-treated and 0.05mg/kg group ($P<0.01$), but not from the 0.10mg/kg or 0.15mg/kg groups. This group first showed statistically significant mechanical hyperalgesia versus controls at day 19 (naïve: 17.2 ± 2.49 g, bortezomib: 9.75 ± 1.36 g), after the 0.10mg/kg and 0.15mg/kg doses showed similar differences (Fig. 1D). However, because of a larger error at the day 12 and 16 time points, the 0.20mg/kg group could not be determined to be significantly different from either saline-treated rats or rats treated with other doses of bortezomib. Significant differences versus saline-treated rats were also observed at days 23, 26, 34, 47, and 54. Peak severity was observed at days 23 and 26 (7.25 and 7.36g). Animals showed highly variable mechanical sensitivity in the time points that followed, but did not show consistent recovery with statistically equivalent behavior versus saline-treated rats until days 63 and 69.

2.2 Thermal, Cold, and Motor Behavior

In thermal testing, both saline and bortezomib -treated groups remained at baseline levels throughout testing until they were sacrificed at day 30, long after significant differences appeared in rats tested for mechanical hyperalgesia (Fig. 2). Similarly, bortezomib-treated animals remained in line with saline-treated counterparts when tested for cold sensitivity throughout the period of testing (Fig. 3). There was one time point in which bortezomib-treated rats scored significantly higher than saline-treated rats, but this score was less than 0.5, indicating on average less than one withdrawal event per test. Peak scores never rose far beyond a score of 1.0. Rotarod testing showed a lack of motor impairment in animals treated with bortezomib, as well (Fig. 4). Although some time points showed average walking times less than the 120 second cutoff time, none of these data points were significant.

2.3 Electrophysiology

WDR neurons in bortezomib-treated rats showed higher acute responses and afterdischarges to mechanical stimuli compared against neurons in control rats (Fig. 5). Spontaneous firing of neurons was negligible in both groups (naïve: 0.036 ± 0.016 spikes/s, bortezomib: 0.13 ± 0.053 spikes/s). Both acute responses to Brush (naïve: 3.6 ± 0.30 spikes/s, bortezomib: 9.1 ± 0.93 spikes/s) and afterdischarges (naïve: 0.090 ± 0.052 spikes/s, bortezomib: 1.6 ± 0.32 spikes/s) were significantly elevated in bortezomib rats. The acute responses to the 0.07g von Frey stimulus were not significantly different in bortezomib rats (naïve: 1.3 ± 0.16 spikes/s, bortezomib: 9.2 ± 0.93 spikes/s), but the afterdischarges to this stimulus were significantly higher (naïve: 0.036 ± 0.036 spikes/s, bortezomib: 0.43 ± 0.16 spikes/s). Neither the acute response to the 1.4g von Frey filament (naïve: 2.7 ± 0.32 spikes/s, bortezomib: 3.5 ± 0.42 spikes/s) nor the afterdischarges (naïve: 0.13 ± 0.056 spikes/s, bortezomib: 0.57 ± 0.15 spikes/s) were significantly different from control rats. The responses to the 60g von Frey filament were significantly higher in bortezomib (naïve: 4.7 ± 0.40 spikes/s, bortezomib: 7.5 ± 0.73 spikes/s), as were the afterdischarges (naïve: 0.20 ± 0.13 spikes/s, bortezomib: 1.2 ± 0.29 spikes/s). Venous clip (light skin compression) responses were

significantly higher in bortezomib (naïve: 5.3 ± 0.77 spikes/s, bortezomib: 9.6 ± 0.67 spikes/s), as were the afterdischarges (naïve: 0.65 ± 0.26 spikes/s, bortezomib: 3.5 ± 0.62 spikes/s). Arterial clip (painful skin compression) responses were significantly higher in bortezomib (naïve: 7.5 ± 0.98 spikes/s, bortezomib: 14 ± 1.2 spikes/s), as were the afterdischarges (naïve: 1.0 ± 0.31 spikes/s, bortezomib: 5.9 ± 0.80 spikes/s).

3. Discussion

Interpretation of dose-response data indicates that a bortezomib-induced peripheral neuropathy will occur even at dose levels lower than therapeutic dose but is maximal for the doses in the therapeutic range. Supramaximal doses of bortezomib did not seem to produce an exacerbation of neuropathy signs above that at the therapeutic range. This parallels the symptoms seen in patients. Treatment-emergent CIPN occurs in 37% of patients within the first five cycles of bortezomib treatment, but frequency plateaus at this point with regard to further treatment cycles (Kane et al., 2006; Richardson et al., 2006; Cavaletti and Jakubowiak, 2010; Broyl, Jongen, Sonneveld, 2012). Dose reduction of bortezomib at the first sign of neuropathy was reported to reduce the severity and risk of further CIPN (Richardson et al., 2006), so it is possible that chemotherapy cycles spread out over a longer period would allow identification of low levels of neuropathy before the threshold is fully reached.

The time course of bortezomib CIPN observed in the present model was similar to the time course seen in the paclitaxel model, which was shown to resolve by day 60 (Cata, Weng, and Dougherty, 2008b) and the oxaliplatin model, which did not resolve until after day 73 (Xiao, Zheng, and Bennett, 2012). This lengthy recovery period is also paralleled by what is seen in patients treated with bortezomib, who may take months to recover from neuropathy by at least one grade (Cavaletti and Jakubowiak, 2010; Broyl, Jongen, Sonneveld, 2012). There must be a persistent signal cascade following bortezomib's activity on its primary targets to produce an effect on this scale, as normal proteasomal activity is restored 48 to 72 hours following treatment (Adams, 2002). Whether this cascade occurs via its activity as a proteasome inhibitor or through a secondary means of action is presently unknown.

In the present study, treatment with bortezomib resulted in the development of mechanical hyperalgesia with an absence of thermal sensitivity, cold sensitivity, or motor impairment. This distinguishes bortezomib from other chemotherapeutic drugs such as paclitaxel, which shows a thermal component in rat models of CIPN (Dina et al., 2001; Cata, Weng, and Dougherty, 2008b), or oxaliplatin, which has components of both thermal and cold hyperalgesia (Joseph and Levine, 2009; Xiao, Zheng, and Bennett, 2012). The observations of the present study do not fully parallel what is seen in patients, who report loss of thermal sensibility and cold hyperalgesia in bortezomib CIPN, as well as increased time to complete a fine motor task (Cata et al., 2007). This mismatch may be a result of physiological differences between humans and rats, or the preclinical tests employed may lack the sensitivity to detect changes in cold sensitivity in this particular model. However, the successful uses of these tests in other rat models of CIPN would argue against the latter. In either case, what causes the apparent behavioral selectivity of this hyperalgesia is unknown and warrants further study, but it does suggest that the possibility that the driving

mechanism behind bortezomib-induced peripheral neuropathy may be distinct from that of other forms of peripheral neuropathy.

Since bortezomib does not cross the blood-brain barrier, it is extremely unlikely that the CNS would be the primary site where bortezomib-induced peripheral neuropathy is initiated but rather includes an effect on primary afferents nerve ending and/or dorsal root ganglion cell bodies. The exact nature of how changes in peripheral nerves or DRG affect the activity of spinal neurons remains to be defined, but the results here show that once engaged altered signaling within the spinal cord likely further contributes to the overall state of neuropathic pain. One possibility is that persistent sensation or signaling from primary afferents could drive central sensitization as seen in other nerve injury models (Rygh et al., 1999; Ji et al., 2003). This would explain the increased spiking frequency during stimulation observed in the present study's electrophysiology data, as well as the persistent afterdischarges observed. Alternatively, spinal glial cells are a target for future study that could contribute to the present study's observed phenotype. These cells are currently thought to have a major role in chronic pain through the release of pro-inflammatory cytokines and chemokines such as IL-1 β , TNF- α , and CCL2 (Clark, Old, and Malcangio, 2013; Ji, Berta, and Nedergaard, 2013). However, an additional maladaptive response that may be seen in spinal glial cells is the dysfunction of astrocytic glutamate transporters, which would account for persistent afterdischarges observed in the present study and be in line with aforementioned plasticity-related theories of chronic pain. Indeed, this involvement of glutamate transporters in the presence of enhanced WDR responses has been observed previously in paclitaxel and cisplatin-treated rats (Cata et al., 2006; Cata, Weng, and Dougherty, 2008a; Zhang et al., 2012).

Little is presently known about how the inhibition of the proteasome by bortezomib results in neuropathic pain, but it is clear from the present study that this drug has mechanistically distinct activity separating it from other chemotherapeutic agents. Namely, bortezomib resulted in mechanical hypersensitivity, increased firing of WDR neurons, and persistent afterdischarges in these cells in the absence of changes to thermal sensitivity, cold sensitivity, or motor ability. Further studies are required to isolate candidate targets in the induction of bortezomib-induced peripheral neuropathy, but the overall downstream mechanism or signal cascade may be similar to that of another pain model if spinal neurons and contributing glial cells display a similar profile of activation between bortezomib-induced peripheral neuropathy and other types of neuropathy.

4. Experimental Procedure

4.1 Animals

A total of 61 male Sprague Dawley rats (Harlan) were used. Animals were housed on a 12hr/12hr light cycle and provided food and water ad libitum throughout the testing period. All efforts were taken to minimize pain and discomfort in animals, and all handling and procedures were approved by the institutional review board and in accordance with institutional ethical standards.

4.2 Drugs

All agents were administered by intraperitoneal (i.p.) injection at in equivalent volumes (0.7mL per injection). Pharmaceutical grade bortezomib (Velcade®, Millennium Pharmaceuticals) was diluted in saline to the desired concentration. Dosages of 0.05mg/kg, 0.10mg/kg, 0.15mg/kg, and 0.20mg/kg per injection were used in the initial behavioral characterization studies. A total of four injections of each dose were administered on days 1, 3, 5, and 7 of each study resulting in cumulative doses of 0.20mg/kg, 0.40mg/kg, 0.60mg/kg, and 0.80mg/kg per treatment. The 0.15mg/kg dose was subsequently defined as the optimal dose in producing the behavioral phenotype that was used in the follow-up neurophysiology studies. Control groups of rats were treated with saline vehicle alone at the same time intervals.

4.3 Mechanical hyperalgesia testing

Sensitivity to mechanical stimuli was assessed using Von Frey filaments as previously described (Boyette-Davis and Dougherty, 2011; Yoon et al., 2013). A range of filaments calibrated to 1g, 4g, 10g, 15g, and 26g of bending force were used for testing. Filaments were applied to the mid-plantar surface of the hindpaw until a bend was observed in the filament and held for approximately 1 second. After a half-hour habituation period, each animal had its mechanical withdrawal threshold for each foot assessed as the lowest filament in the series at which the animal responded to at least 50% of six applications. Animals were tested for baseline response just prior to their first injection of drug (day 1) and the days after each injection (days 2, 4, 6, and 8). Following this, rats were tested for mechanical threshold twice weekly for one month, then once weekly until recovery from the hyperalgesia phenotype, assessed as a return to baseline withdrawal threshold.

4.4 Thermal hyperalgesia testing

Thermal sensitivity in rats was tested using a Hargreaves testing apparatus (Ugo Basile). An infrared beam was directed to the mid-plantar surface of each hindpaw, and the latency to withdrawal was measured. This was repeated for three trials per paw with a 20 second cutoff to prevent tissue damage. Baseline beam intensity was set to evoke a baseline response between 10-12 seconds. Rats were tested at time points corresponding to those of dose response testing until day 30.

4.5 Cold sensitivity testing

Rats were tested for cold sensitivity via scored responses to application of acetone. For each trial, 50µL of acetone was applied to the mid-plantar surface of each hindpaw using a calibrated pipette. The behavior of the rat was observed and scored for 20 seconds following this application. A score of 1 was assigned for each rapid withdrawal or flicking of the foot. A score of 2 indicated prolonged withdrawal, and a score of 3 indicated licking of the hindpaw. Trials were conducted three times per hindpaw, for a total of six trials per testing period. Cold sensitivity testing was conducted at the same time points as thermal testing.

4.6 Motor impairment testing

The potential for motor impairment due to chemotherapy treatment was assessed by rotarod assay as previously described (Cata, Weng, and Dougherty, 2008b). A rotating wheel was set to increase over time from a speed of 4rpm to 40rpm. Each animal was placed on this accelerating wheel and allowed to walk for 120 seconds or until it fell off of the wheel, at which point the rotating wheel would shut off automatically. Three trials were recorded per animal per time point with a 5 minute resting period between trials. Time points corresponded to those of thermal testing.

4.7 In vivo electrophysiology

All rats used for *in vivo* electrophysiology treated with bortezomib had confirmed behavioral hypersensitivity to chemotherapy and were compared to saline-treated controls. Rats were anesthetized using urethane (1.5g/kg i.p.) and anesthetic depth was verified by toe pinch for loss of nociceptive reflexes with supplemental anesthetic given as needed. The L5-6 spinal cord was exposed via laminectomy and the animal then mounted into a stereotactic frame. The spinal cord was covered with agar with an opening to allow electrode access that was kept filled with saline. A parylene-coated tungsten filament electrode (resistance 1.4-1.8M Ω , Microprobes Inc.) was advanced into the spinal cord using a hydraulic Microdrive. Cells were isolated using mechanical stimulation of the paw. Wide dynamic range (WDR) neurons responding in graded fashion to innocuous and noxious stimuli achieving a signal to noise ratio greater than 5 were selected for study.

Assessment of neuronal activity began with recording of 60 seconds spontaneous activity. Mechanical stimuli were then applied for 10 seconds each with 30 second inter-stimulus intervals. The stimuli included camel hair brush (1 application/second), 0.07g von Frey filament (1 application/second), 1.4g von Frey filament (1 application/second), 60g von Frey filament (1 application/second), venous clip (continual application), and arterial clip (continual application). Spike2 software was used to capture spikes and for off-line analysis of stimulus response frequencies and afterdischarge rates. The 5 seconds following each stimulus were used for analysis of afterdischarges.

4.8 Statistics

For all measurements in both behavior testing and electrophysiology, each representative data point was calculated as the mean value for a given group at the time point represented. Error bars were then calculated as standard error of the mean, and significance was determined using a Mann-Whitney test ($\alpha = 0.05, 0.025, 0.01$). Additionally, a one-way ANOVA with a post-hoc Tukey test was used in mechanical behavior testing across doses to determine whether the observed behavior differed versus control and between other doses ($P = 0.05, 0.01$).

Acknowledgments

This work was supported by NIH grant NS046606 and NCI grant CA124787.

References

- Adams J, Palombella VJ, Sausville EA, Johnson J, Destree A, Lazarus DD, Maas J, Pien CS, Prakash S, Elliott PJ. Proteasome Inhibitors: a novel class of potent and effective antitumor agents. *Cancer Res.* 1999; 59:2615–2622. [PubMed: 10363983]
- Adams J. Development of the proteasome inhibitor PS-341. *Oncologist.* 2004; 7:9–16. [PubMed: 11854543]
- Adams J, Kauffman M. Development of the proteasome inhibitor Velcade (Bortezomib). *Cancer Invest.* 2004; 22:304–311. [PubMed: 15199612]
- Aghajanian C, Soignet S, Dizon DS, Pien CS, Adams J, Elliott PJ, Sabbatini P, Miller V, Hensley ML, Pezzulli S, Canales C, Daud A, Spriggs DR. A phase I trial of the novel proteasome inhibitor PS341 in advanced solid tumor malignancies. *Clin Cancer Res.* 2002; 8:2505–2511. [PubMed: 12171876]
- Boyette-Davis J, Dougherty PM. Protection against oxaliplatin-induced mechanical hyperalgesia and intraepidermal nerve fiber loss by minocycline. *Exp Neurol.* 2011; 229:353–357. [PubMed: 21385581]
- Boyette-Davis JA, Cata JP, Zhang H, Driver LC, Wendelschafer-Crabb G, Kennedy WR, Dougherty PM. Follow-up psychophysical studies in bortezomib-related chemoneuropathy patients. *J Pain.* 2011; 12:1017–1024. [PubMed: 21703938]
- Boyette-Davis JA, Cata JP, Driver LC, Novy DM, Bruel BM, Mooring DL, Wendelschafer-Crabb G, Kennedy WR, Dougherty PM. Persistent chemoneuropathy in patients receiving the plant alkaloids paclitaxel and vincristine. *Cancer Chemother Pharmacol.* 2012; 71:619–626. [PubMed: 23228992]
- Broyl A, Jongen JLM, Sonneveld P. General aspects and mechanisms of peripheral neuropathy associated with bortezomib in patients with newly diagnosed multiple myeloma. *Semin Hematol.* 2012; 49:249–257. [PubMed: 22726548]
- Cata JP, Weng HR, Chen JH, Dougherty PM. Altered discharges of spinal wide dynamic range neurons and down-regulation of glutamate transporter expression in rats with paclitaxel-induced hyperalgesia. *Neuroscience.* 2006; 138:329–338. [PubMed: 16361064]
- Cata JP, Weng HR, Burton AW, Villareal H, Giral S, Dougherty PM. Quantitative sensory findings in patients with bortezomib-induced pain. *J Pain.* 2007; 8:296–306. [PubMed: 17175202]
- Cata JP, Weng HR, Dougherty PM. Behavioral and electrophysiological studies in rats with cisplatin-induced chemoneuropathy. *Brain Res.* 2008; 1230:91–98. [PubMed: 18657527]
- Cata JP, Weng HR, Dougherty PM. The effects of thalidomide and minocycline on taxol-induced hyperalgesia in rats. *Brain Res.* 2008; 1229:100–110. [PubMed: 18652810]
- Cavaletti G, Jakubowiak AJ. Peripheral neuropathy during bortezomib treatment of multiple myeloma: a review of recent studies. *Leuk Lymphoma.* 2010; 51:1178–1187. [PubMed: 20497001]
- Clark AK, Old EA, Malcangio M. Neuropathic pain and cytokines: current perspectives. *J Pain Res.* 2013; 6:803–814. [PubMed: 24294006]
- Dina OA, Chen X, Reichling D, Levine JD. Role of protein kinase C epsilon and protein kinase A in a model of paclitaxel-induced painful peripheral neuropathy in the rat. *Neuroscience.* 2001; 108:507–515. [PubMed: 11738263]
- Dougherty PM, Cata JP, Burton AW, Vu K, Weng HR. Dysfunction in multiple primary afferent fiber subtypes revealed by quantitative sensory testing in patients with chronic vincristine-induced pain. *J Pain Symptom Manage.* 2007; 33:166–179. [PubMed: 17280922]
- Hideshima T, Richardson P, Chauhan D, Palombella VJ, Elliott PJ, Adams J, Anderson KC. The proteasome inhibitor PS-341 inhibits growth, induces apoptosis, and overcomes drug resistance in human multiple myeloma cells. *Cancer Res.* 2001; 61:3071–3076. [PubMed: 11306489]
- Hideshima T, Mitsiades C, Akiyama M, Hayashi T, Chauhan D, Richardson P, Schlossman R, Podar K, Munshi NC, Mitsiades N, Anderson KC. Molecular mechanisms mediating antimyeloma activity of proteasome inhibitor PS-341. *Blood.* 2003; 101:1530–1534. [PubMed: 12393500]
- Ji RR, Kohno T, Moore KA, Woolf CJ. Central sensitization and LTP: do pain and memory share similar mechanisms? *Trends Neurosci.* 2003; 26:696–705. [PubMed: 14624855]
- Ji RR, Berta T, Nedergaard M. Glia and pain: is chronic pain a gliopathy? *Pain.* 2013; 154(Suppl 1):S10–28. [PubMed: 23792284]

- Joseph EK, Levine JD. Comparison of oxaliplatin- and cisplatin-induced painful peripheral neuropathy in the rat. *J Pain*. 2009; 10:534–541. [PubMed: 19231296]
- Kane RC, Farrell AT, Sridhara R, Pazdur R. United States Food and Drug Administration approval summary: bortezomib for the treatment of progressive multiple myeloma after one prior therapy. *Clin Cancer Res*. 2006; 12:2955–2960. [PubMed: 16707588]
- Kaufman JL, Nooka A, Vrana M, Gleason C, Heffner LT, Lonial S. Bortezomib, thalidomide, and dexamethasone as induction therapy for patients with symptomatic multiple myeloma: a retrospective study. *Cancer*. 2010; 116:3143–3151. [PubMed: 20564642]
- Landowski TH, Megli CJ, Nullmeyer KD, Lynch RM, Dorr RT. Mitochondrial-mediated dysregulation of Ca²⁺ is a critical determinant of Velcade (PS-341/Bortezomib) cytotoxicity in myeloma cell lines. *Cancer Res*. 2005; 65:3828–3836. [PubMed: 15867381]
- Richardson PG, Briemberg H, Jagannath S, Wen PY, Barlogie B, Berenson J, Singhal S, Siegel DS, Irwin D, Schuster M, Srkalovic G, Alexanian R, Rajkumar SV, Limentani S, Alsina M, Orlowski RZ, Najarian K, Esseltine D, Anderson KC, Amato AA. Frequency, characteristics, and reversibility of peripheral neuropathy during treatment of advanced multiple myeloma with bortezomib. *J Clin Oncol*. 2006; 24:3113–3120. [PubMed: 16754936]
- Rygh LJ, Svendsen F, Hole K, Tjølsen A. Natural noxious stimulation can induce long-term increase of spinal nociceptive responses. *Pain*. 1999; 82:305–310. [PubMed: 10488682]
- San Miguel JF, Schlag R, Khuageva NK, Dimopoulos MA, Shpilberg O, Kropff M, Spicka I, Petrucci MT, Palumbo A, Samoilova OS, Dmoszynska A, Abdulkadyrov KM, Schots R, Jiang B, Mateos MV, Anderson KC, Esseltine DL, Liu K, Cakana A, van de Velde H, Richardson PG. VISTA Trial Investigators. Bortezomib plus melphalan and prednisone for initial treatment of multiple myeloma. *N Engl J Med*. 2008; 359:906–917. [PubMed: 18753647]
- Voorhees PM, Dees EC, O'Neil B, Orlowski RZ. The proteasome as a target for cancer therapy. *Clin Cancer Res*. 2003; 9:6316–6325. [PubMed: 14695130]
- Xiao WH, Zheng H, Bennett GJ. Characterization of oxaliplatin-induced chronic painful peripheral neuropathy in the rat and comparison with the neuropathy induced by paclitaxel. *Neuroscience*. 2012; 203:194–206. [PubMed: 22200546]
- Yoon SY, Robinson CR, Zhang H, Dougherty PM. Spinal astrocyte gap junctions contribute to oxaliplatin-induced mechanical hypersensitivity. *J Pain*. 2013; 14:205–214. [PubMed: 23374942]
- Zhang H, Yoon SY, Zhang H, Dougherty PM. Evidence that spinal astrocytes but not microglia contribute to the pathogenesis of paclitaxel-induced painful neuropathy. *J Pain*. 2012; 13:293–393. [PubMed: 22285612]

Highlights

- Bortezomib-treated rats develop threshold-dependent mechanical hyperalgesia
- No changes in thermal sensitivity, cold sensitivity, or motor function were observed
- Spinal WDR neurons showed increased firing and persistent after-discharges

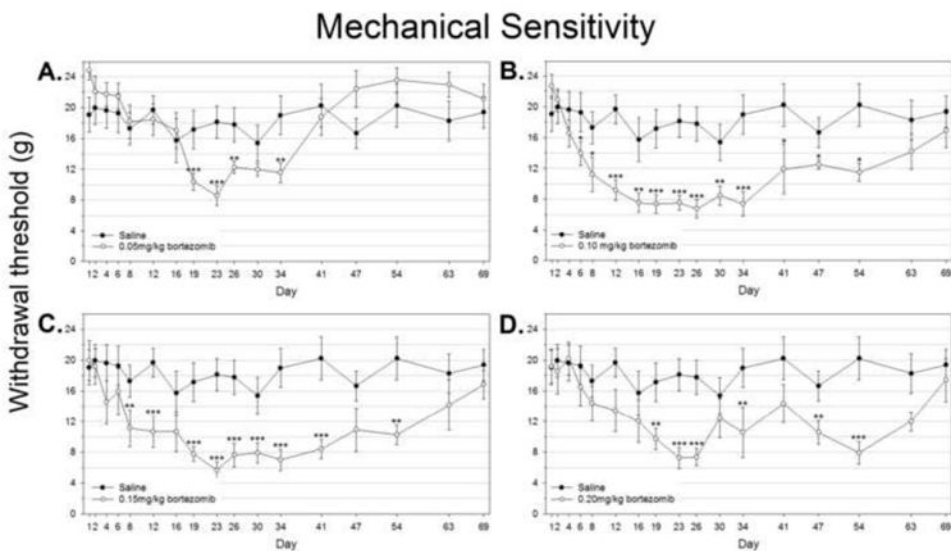


Figure 1. Bortezomib produces mechanical hyperalgesia in rats. Mechanical sensitivity was assessed by responses to mid-plantar application of von Frey filaments over time. **A)** Saline treated control group vs. rats treated with 0.05mg/kg bortezomib **B)** Saline treated control group vs. rats treated with 0.10mg/kg bortezomib **C)** Saline treated control group vs. rats treated with 0.15mg/kg bortezomib **D)** Saline treated control group vs. rats treated with 0.20mg/kg bortezomib

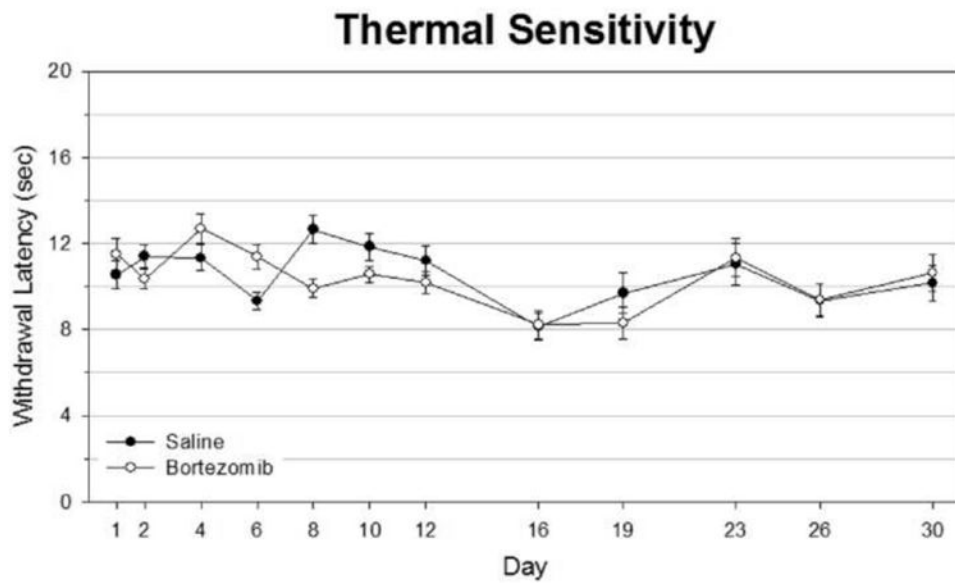


Figure 2.

Bortezomib does not produce thermal hyperalgesia in rats. Thermal sensitivity was assessed via Hargreaves test, using a focused infrared beam with an automatic cutoff when interrupted by movement of the rat's foot. Infrared intensity was calibrated such that animals would respond on average after 10-12 seconds of continuous exposure at baseline, and this intensity was maintained throughout testing. Withdrawal latencies were obtained three times per foot per rat per time point. Neither saline-treated nor bortezomib-treated rats consistently showed an average withdrawal latency significantly below 10 seconds throughout testing, which falls within baseline range.

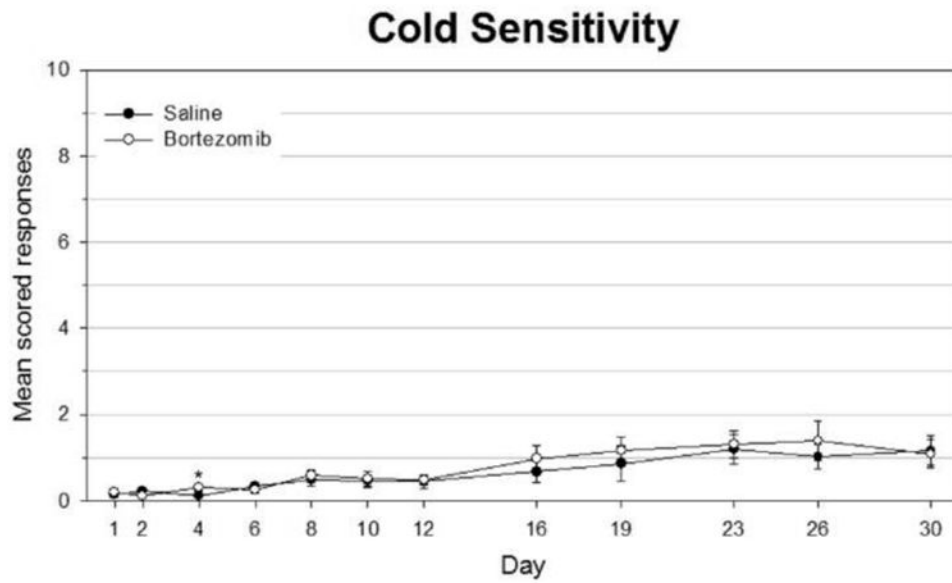


Figure 3.

Bortezomib-treated rats did not develop cold hypersensitivity. Cold stimuli were simulated by applying acetone to the mid-plantar surface of each hindpaw. Responses were scored for each of three trials per foot per rat per time point. Scores were based on behavior in the 20 seconds following application of acetone.

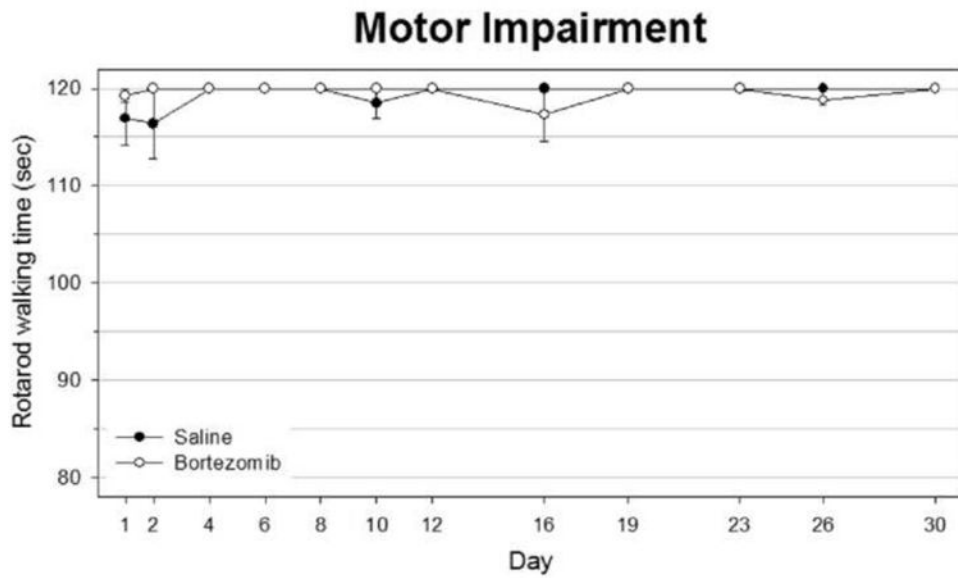


Figure 4. Bortezomib-treated rats did not develop motor impairment. Rats were allowed to walk on a rotarod that slowly accelerated from 4-40rpm. Walking time was recorded either until the rat fell from the wheel or until a 120 second cutoff was reached.

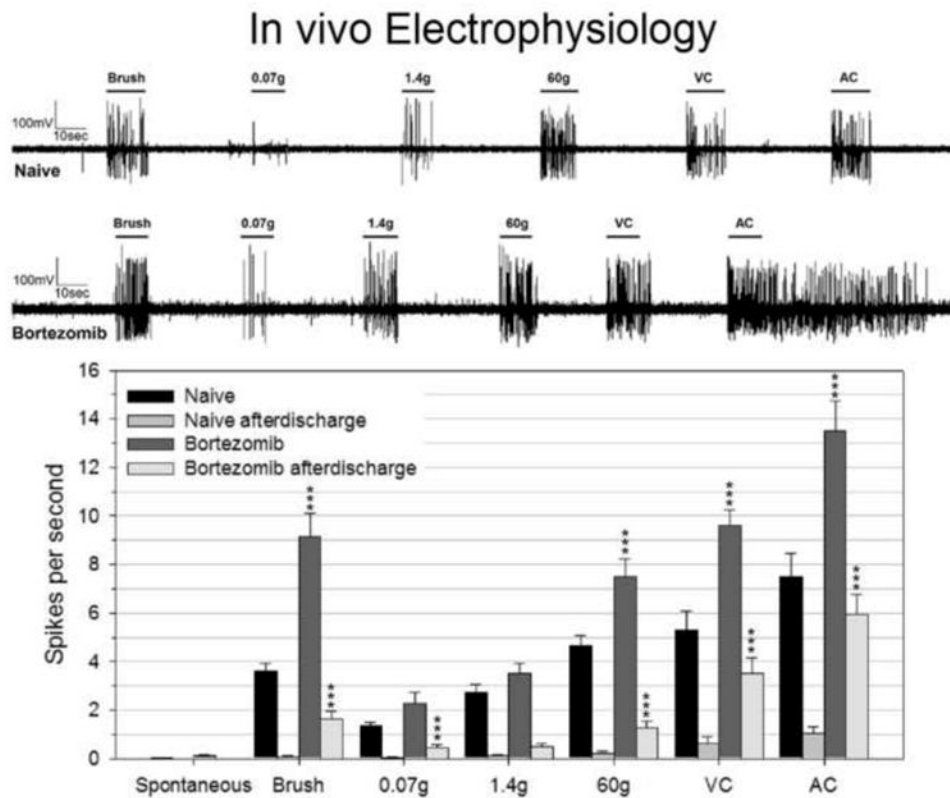


Figure 5.

In vivo electrophysiology was used to find the spikes generated per second from wide dynamic range neurons during and immediately following different types of stimuli. Average spikes per second in bortezomib rat cells were compared against those for naïve rats for each stimulus type, and afterdischarges in bortezomib rat cells were compared against afterdischarges for naïve rats for each stimulus type. Representative analog recordings data for naïve and bortezomib-treated rat neurons are pictured at the top of the figure with the horizontal lines indicating the type and duration of stimuli during each recording. The bar graphs at the bottom summarize the grouped data.